Research Square

Preprints are preliminary reports that have not undergone peer review.
They should not be considered conclusive, used to inform clinical practice,
or referenced by the media as validated information.

Post-Stack Seismic Modelling and Reservoir Mapping in Uzondu Field, Niger Delta Basin, Nigeria

Uzochukwu Chioma Omoja

uc.omoja@unizik.edu.ng

Nnamdi Azikiwe University

Gabriel Ndubuisi Egwuonwu

Nnamdi Azikiwe University

Francis Omonefe

Federal University Otuoke

Chukwudike Gabriel Okeugo

University of Nigeria

Research Article

Keywords:

Posted Date: May 28th, 2026

DOI: https://doi.org/10.21203/rs.3.rs-9613573/v1

License: This work is licensed under a Creative Commons Attribution 4.0 International License.
Read Full License

Additional Declarations: No competing interests reported.

Post-Stack Seismic Modelling and Reservoir Mapping in *Uzondu* Field, Niger Delta Basin, Nigeria

Uzochukwu Chioma Omoja[1], Gabriel Ndubuisi Egwuonwu[1], Francis Omonefe[2] and Chukwudike Gabriel Okeugo[3]

[1]*Department of Physics and Industrial Physics, Nnamdi Azikiwe University, Awka, Nigeria*
[2]*Department of Geology, Federal University, Otuoke, Bayelsa, Nigeria*
[3]*Department of Geology, University of Nigeria, Nsukka*
Corresponding Author Email: uc.omoja@unizik.edu.ng

Abstract

Post-stack seismic modelling was applied to the Uzondu Field, Niger Delta Basin, to quantitatively delineate reservoir geometry and evaluate hydrocarbon potential. The study integrates 2D seismic data, well logs, and check-shot data to constrain elastic property estimation and improve subsurface characterization. Two hydrocarbon-bearing sandstone reservoirs (Zones A and B) were mapped within the Agbada Formation using seismic-to-well calibration and inversion workflows. Fluid replacement modelling (FRM) based on Biot-Gassmann theory was used to simulate elastic responses under varying saturation conditions, while missing S-wave logs were generated using Castagna's mudrock relation. AVO modelling and synthetic seismogram generation show improved seismic-to-well correlation after cross-correlation, confirming the reliability of the derived elastic parameters. Quantitative results shows that the reservoir interval is characterized by P-impedance values of ~21,000 to 24,000 ft/s·g/cc, S-impedance values of ~9,000 to 13,000 ft/s·g/cc, density values of ~2.1 to 2.3 g/cc, and Poisson's ratio ranging from ~0.30 to 0.36. These values are consistently lower than surrounding formations, where P-impedance exceeds ~26,000 ft/s·g/cc, S-impedance exceeds ~14,000 ft/s·g/cc, and Poisson's ratio is greater than ~0.40. The observed impedance contrasts generate strong reflection amplitudes and clearly define the reservoir top and base between Horizon 1 and 3 as well as Horizon 3 and 4. The lateral continuity of low-impedance zones tells a well-developed, laterally extensive sandstone bodies, while AVO responses demonstrate sensitivity to fluid variations, supporting hydrocarbon presence. The integrated workflow reduces interpretation uncertainty and provides a robust framework for reservoir delineation, facies discrimination, and field development planning in complex deltaic systems.

1. Introduction

The Niger Delta Basin represents one of the most prolific hydrocarbon provinces globally, characterized by a tripartite stratigraphy comprising the Akata, Agbada, and Benin Formations[1-3]. Hydrocarbon accumulation is predominantly controlled by growth fault systems, rollover anticlines, and shale diapirism, which introduce significant structural complexity and reservoir compartmentalization [4-5]. Traditional seismic interpretation methods, largely structure-driven, have proven insufficient for reliable fluid and lithology prediction. Amplitude anomalies such as

bright spots are often ambiguous due to tuning effects, lithologic variations, and noise contamination [6-7].

In mature hydrocarbon provinces such as the Niger Delta Basin, complex stratigraphic architecture, rapid facies changes, and vertical stacking of sand–shale sequences introduce significant uncertainty in reservoir continuity and geometry. Thus, accurate reservoir delineation in a deltaic basins such as Niger Delta requires effective integration of seismic interpretation and well data [8-10]. Seismic reservoir characterization needs to integrate all the geophysical and geological data to reduce exploration and production risks in the oil and gas industry. Seismic data, when properly processed and calibrated with well information, provide a powerful tool for mapping reservoir distribution and thickness variation across the field.

Seismic inversion converts seismic reflection data into quantitative rock-property models such as acoustic impedance, elastic impedances, density, Vp/Vs that can be related to lithology and fluids [11]. This reduces interpretation ambiguity by linking seismic responses to physical rock properties [12]. Two broad classes are commonly used: post-stack (acoustic) inversion, which yields acoustic impedance from stacked seismic, and pre-stack (elastic) inversion, which recovers P-impedance, S-impedance and density for fluid discrimination when calibrated to well data and rock physics models [13-14]. Acoustic impedance inversion converts band-limited seismic reflectivity into impedance contrasts that correlate with rock properties. Different seismic inversion techniques have been developed to convert seismic reflection data into layer reservoir properties to enhance our understanding of the subsurface geology [15-19], improve the accuracy of reservoir models, identifying potential hydrocarbon zones, and optimizes well placement and production strategies [12,20-23].

In the Niger Delta, both deterministic and geostatistical (stochastic) inversion workflows have been applied to improve mapping of thin sand bodies, separate fluid from lithologic effects, and reduce uncertainty in prospect ranking. Case studies show consistent benefits when inversion is constrained by well logs and rock-physics analysis [24-27]. The reliability of seismic inversion can all reduce by bandwidth/low-frequency content, seismic noise, velocity uncertainty, structural complexity (faulting, diapirs) and sparse well control. In the Niger Delta, inversion must be tightly calibrated to well logs, using realistic rock-physics models, and preferably include stochastic realizations to quantify uncertainty [13-14,24-25,28-30].

Post-stack seismic modelling plays a critical role in reservoir characterization by enhancing reflector continuity and improving interpretability of stratigraphic horizons [31]. Stacked seismic sections derived from processed prestack data offer improved signal-to-noise ratio and clearer representation of subsurface reflectors, enabling reliable horizon picking and reservoir correlation. In this study, post-stack seismic modelling was applied to *Uzondu* Field using stacked seismic sections and well log information from Well *Uzondu*_A. Two hydrocarbon-bearing sandstone reservoirs (Zones A and B), were mapped across the seismic volume. The objective of this study is to establish a reliable seismic to well framework for reservoir delineation, quantify lateral continuity, and define reservoir geometry within the field.

2. Geological Setting

Uzondu Field is located in the south-south region of Nigeria within the onshore Niger Delta province [32-33]. The study area lies between approximately 6°58′30″E to 7°1′30″E longitude and 4°32′00″N to 4°33′30″N latitude, forming a rectangular boundary defined for systematic investigation (Fig. 1). The New Calabar River traverses the area from north to south, dividing it into eastern and western sections, while an additional water channel occurs along the eastern margin. These hydrological features are expected to influence surface runoff, groundwater recharge, and subsurface flow dynamics. Five wells (Wells A - E) are spatially distributed across the area to ensure representative coverage on both sides of the river. Central wells are positioned near drainage features, whereas others extend toward the boundaries, enabling comparative assessment of spatial variability. Minor road networks provide accessibility within the area.

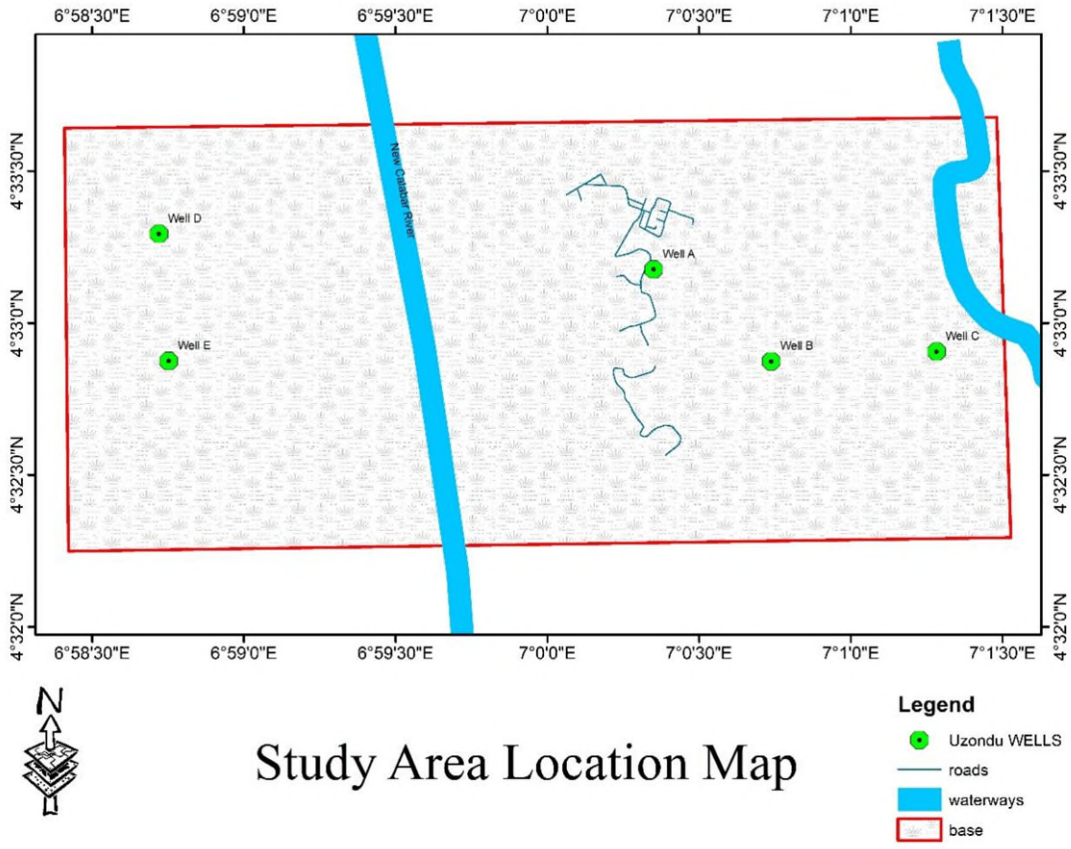


Fig. 1: Study Area map

The Niger Delta Basin represents a major Tertiary clastic wedge deposited in fluvial, deltaic, and shallow marine environments. The basin is characterized by thick sequences of interbedded sands and shales, forming vertically stacked reservoir units separated by shale intervals [2-4,34-35]. The principal reservoir-bearing unit in the subsurface Niger Delta is the Agbada Formation, which consists of alternating sandstone and shale facies deposited in paralic to delta-front environments. Sandstone

reservoirs typically occur as laterally continuous bodies but may exhibit thickness variations due to depositional and compaction processes. This stratigraphic framework provides the geological basis for seismic reflector development and reservoir mapping.

2.1 Lithological setting of the study area

The alluvium unit (Qal) occupies the entire portion of the study area, particularly inland and along river courses (Fig. 2). These deposits consist mainly of unconsolidated sands, silts, clays, and minor gravels transported and deposited by fluvial systems. The widespread occurrence of Qal indicates active sediment reworking by rivers and creeks, consistent with the low-lying, swampy terrain of the Niger Delta. These sediments are typically heterogeneous, with variable grain sizes, and may locally host shallow aquifers.

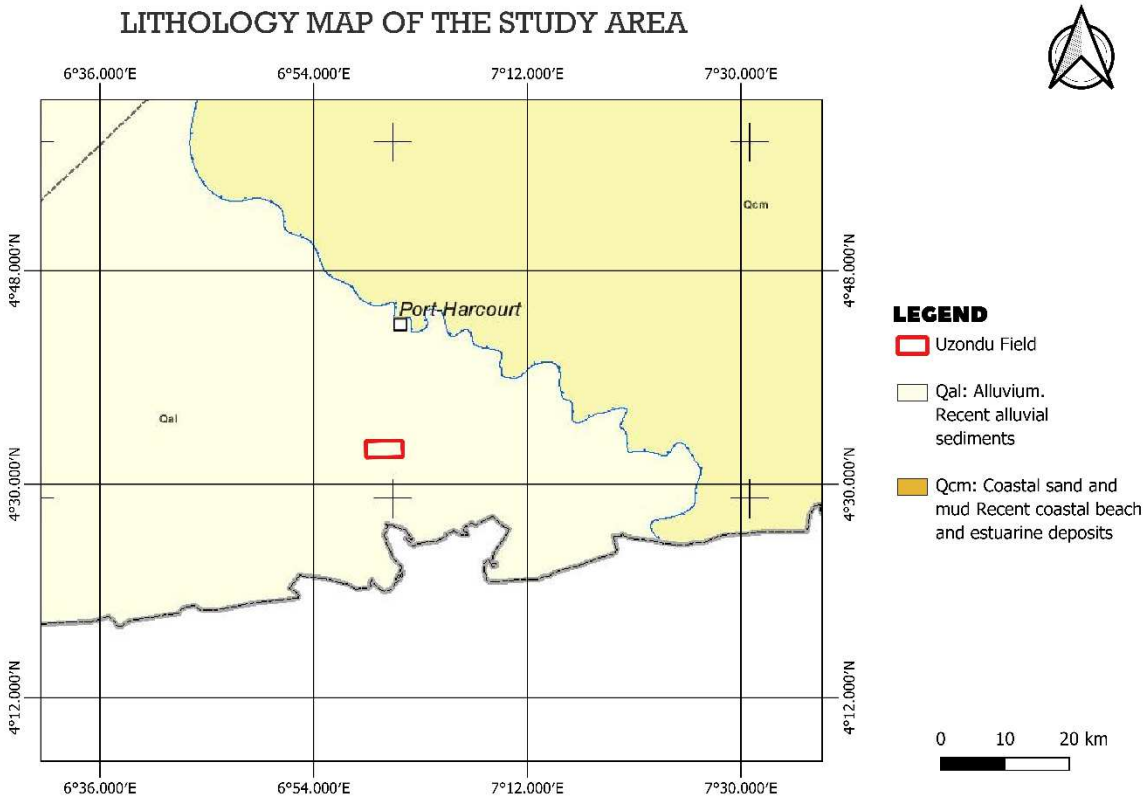


Fig 2: Lithology map of the study area showing the spatial distribution of Quaternary lithologic units, (Qal) and coastal sand and mud deposits (Qcm), with the Uzondu Field highlighted within the fluvio - deltaic setting of the Niger

The coastal sand and mud unit (Qcm) dominates the eastern part of the map and extends toward the coastal margin. This unit represents recent coastal beach, tidal flat, and estuarine deposits, composed of fine- to medium-grained sands interbedded with muds and silts. The Qcm unit reflects strong marine and tidal influences and marks

the transition between fluvial and shallow marine environments. These sediments are generally poorly consolidated and are associated with high porosity and permeability variations due to frequent changes in depositional energy.

The spatial distribution of these lithologic units indicates a fluvio–deltaic depositional regime, where sedimentation is controlled by river discharge, tidal action, and relative sea-level changes. Such environments favor rapid lateral and vertical facies changes, which have important implications for subsurface reservoir heterogeneity in the Niger Delta Basin.

3. Data and Methodology

The dataset used for this study comprises of 2D seismic volume (pre-stack), Well log data and Checkshot data (for time-depth calibration) made available by Shell Petroleum Development Company of Nigeria Ltd (SPDC). The Hampson-Russell software (HRS 10.6) was used for the analysis. The AVO program was used to perform the AVO modeling. P-wave log, S-wave log and density log were required to define the AVO model but S-wave log was not available in the given well data for this study. Hence, S-wave log was then created using Castagna's mudrock equation [36] which relates S-wave and P-wave velocity by a linear eqaution given as

$$S-wave = C_1 * P-wave + C_2 \quad (1)$$

Where C_1 and C_2 are constant whose values are given as 0.86190 and -1172.00000 respectively.

Poisson's ratio log was created in the process. Since Castagna's equation (1) is valid only for the wet background shale. A different calculation to model the gas sand within the target zone was used. Fluid replacement modeling (FRM) was employed using Biot - Gassman's equation [37] which is given as:

$$K_{sat} = K_{dry} + \frac{\left(1-\frac{K_{dry}}{K_m}\right)}{\phi\frac{1}{K_{fl}}+\frac{1-\phi}{K_m}+\frac{K_{dry}}{K_m^2}} \quad (2)$$

Where K=bulk modulus, sat=saturated, dry=dry frame, m=rock matrix, fl=fluid and ϕ=porosity.

Three new logs viz P-wave log (i.e. P-wave_1_FRM), the Density log (Density_1_FRM) and the S-wave log (S-wave_Castagna_FRM); were created in the process which was used to calculate the new synthetic.

With the P-wave log, density log and created S-wave log in place, an offset - dependent synthetic seismogram was created by Reading in seismic data; processing CDP stack of seismic data; extracting statistical wavelet from the CDP stack; performing log correlation and processing a super gather from the original seismic data

The seismic data was read into the AVO modelling window and AVO processing on the Seismic Data was carried out. Four(4) different horizons (1-4) was picked which enabled us to map out the top and base of reservoirs A and B. The super gather created form part of the AVO process. The data was further preconditioned using the

super gather as the input volume for muting and trim statics (Fig. 3). Volumes of acoustic impedance, density, and possion ratio was created using the post-stacked and two reservoirs(A and B) were identified.

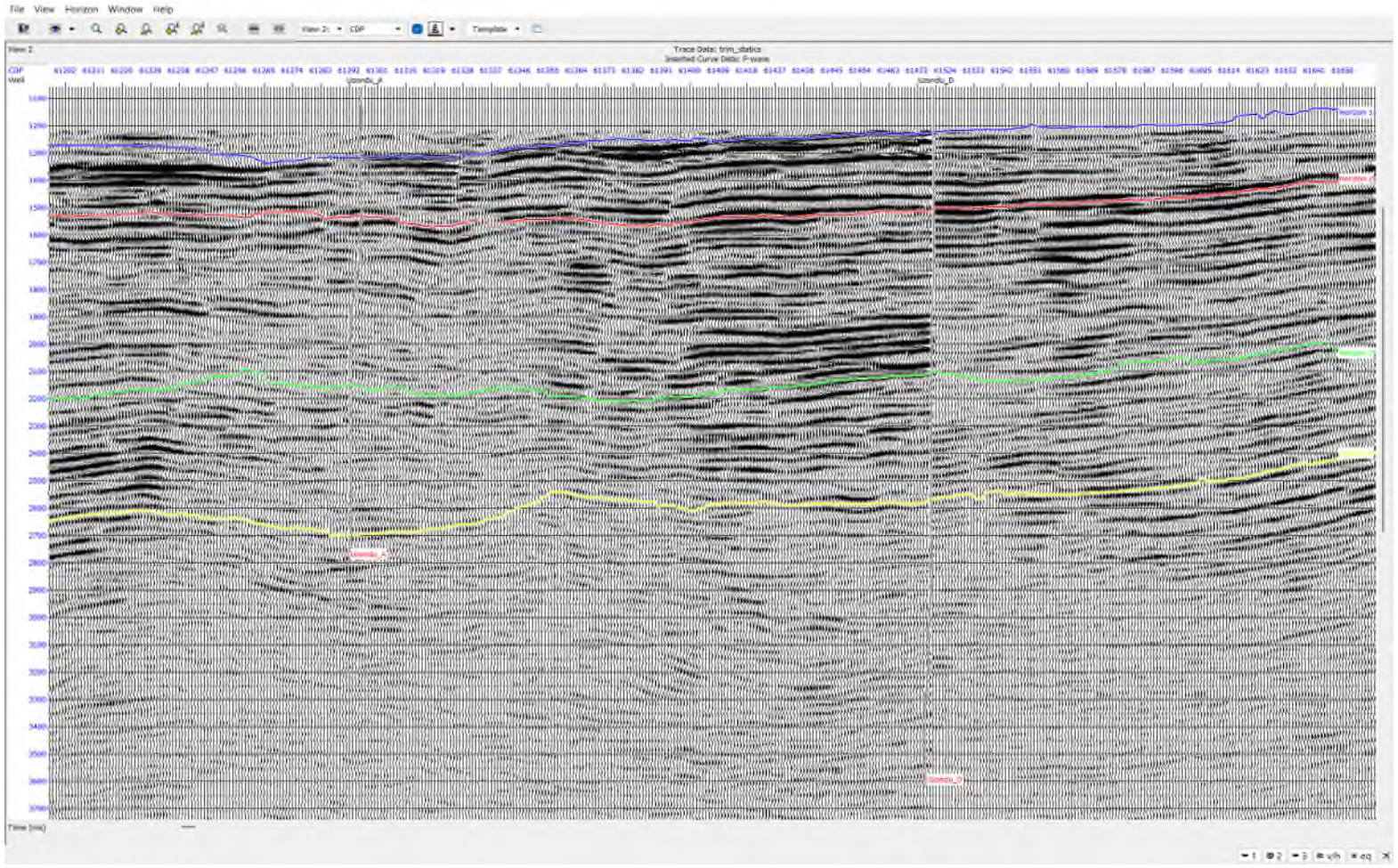


Fig. 3. Final processed data with horizons (after Muting and Trim Statics)

4. Results and Discussion

4.1 Amplitude Versus Offset (AVO) modelling

Amplitude Versus Offset (AVO) modelling was carried out to investigate the elastic response of the identified reservoirs and to establish a robust link between well-log derived rock properties and seismic amplitudes. The modelling process began with the display of a selected portion of the processed seismic data within the AVO modelling window, as shown in Fig. 4. This window provided a suitable framework for integrating seismic gathers, well logs, and synthetic responses, allowing detailed analysis of amplitude variations with offset and angle.

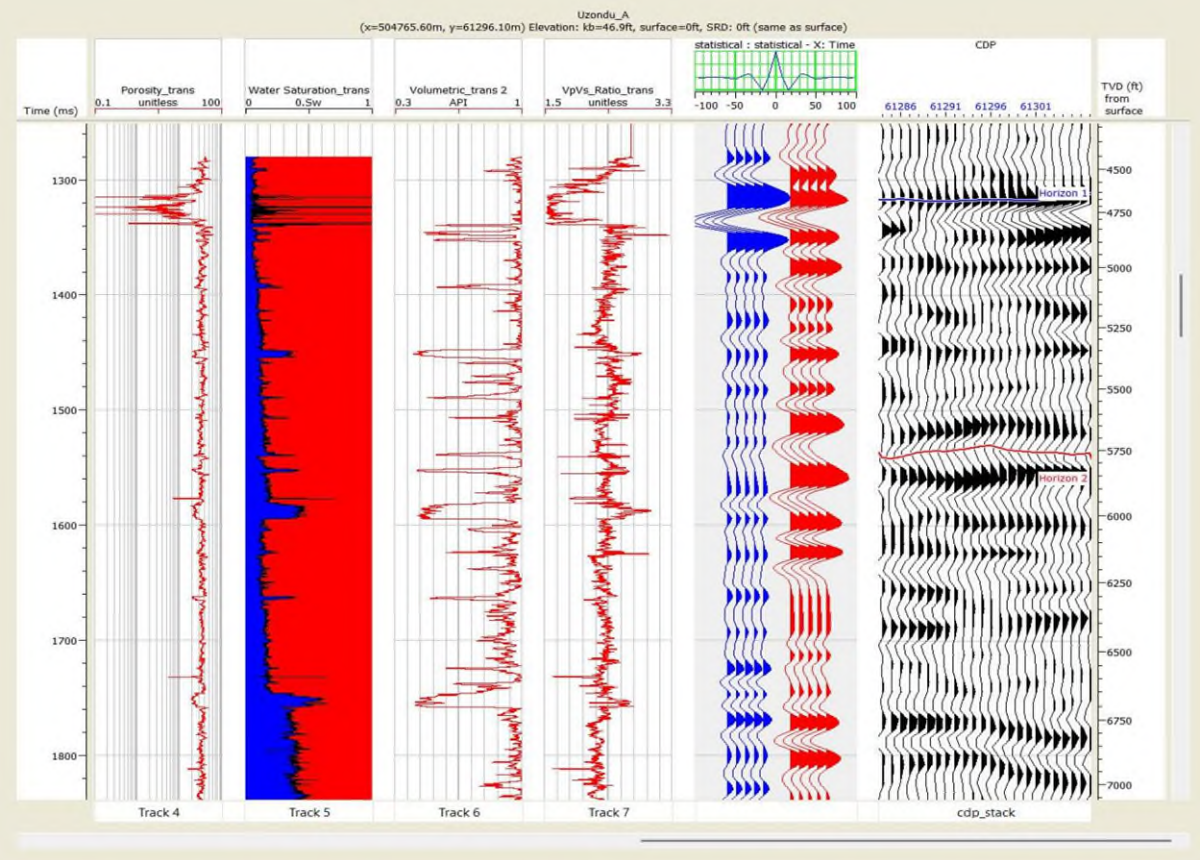


Fig 4: A portion of seismic data displayed in the AVO modeling window

A seismic-to-well tie was first performed using the check-shot corrected sonic and density logs to generate an initial synthetic seismogram. Fig. 5 shows the seismic-to-well tie before correlation, where noticeable misties exist between the synthetic trace and the real seismic data. These discrepancies are attributed to residual time shifts, wavelet phase differences, and local velocity uncertainties. Cross-correlation analysis was applied which improved the alignment, resulting in a time shift that maximized the correlation coefficient between the synthetic and seismic traces.

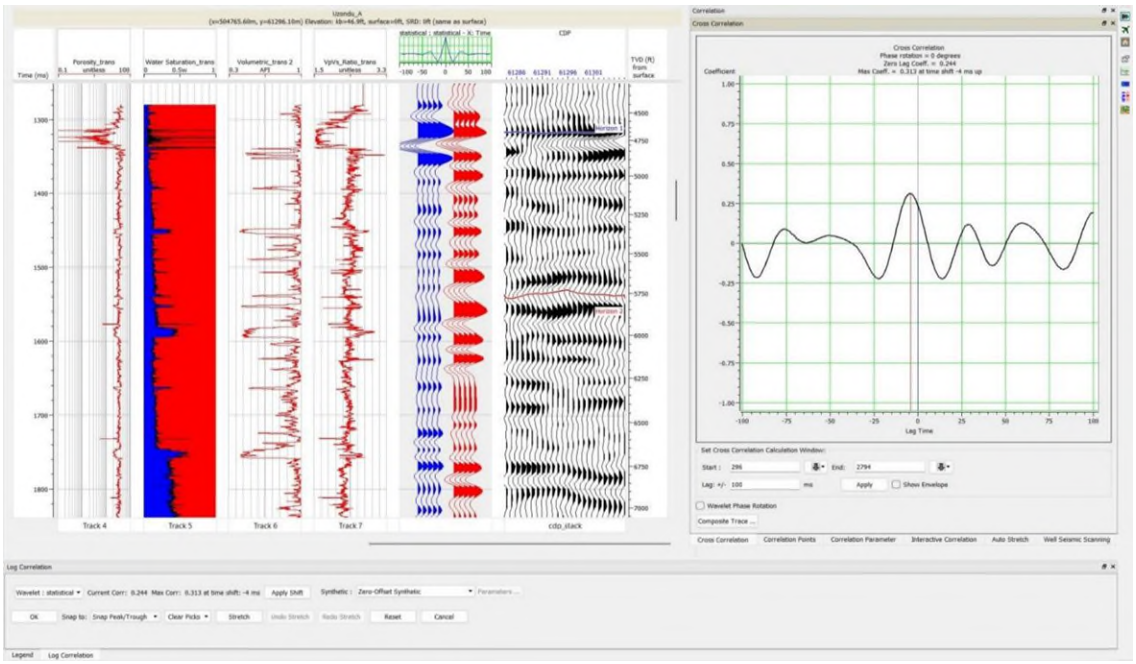


Fig 5: Seismic to well tie before correlation

The improved seismic-to-well tie after correlation is shown in Fig. 6. The synthetic seismogram showed a much better alignment with the seismic reflections, particularly at the key reservoir horizons. The increase in correlation coefficient indicates a reliable tie, confirming that the well-log derived elastic properties adequately represent the seismic response at the well location. This step was critical, as accurate seismic-to-well calibration directly influences the reliability of subsequent AVO and inversion analyses.

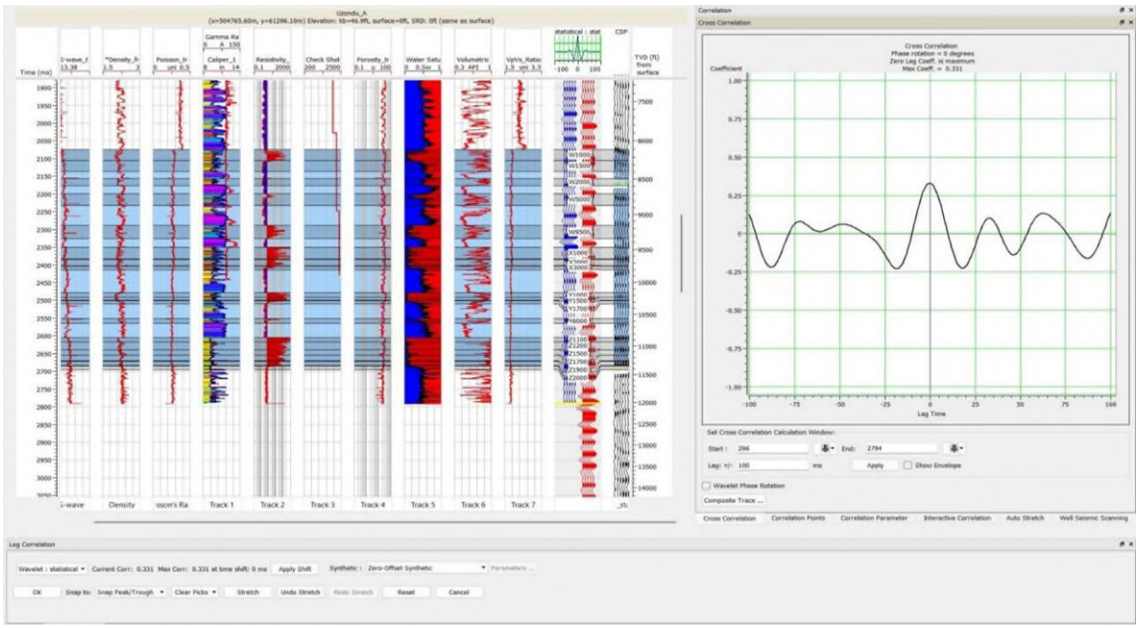


Fig. 6: seismic to well tie after correlation

Following the well tie, a statistical wavelet was extracted from the seismic data at the relevant CDP location, as illustrated in Fig. 7. The extracted wavelet was presented in both the time domain and frequency spectrum. The time-domain wavelet exhibits a zero-phase character, which is desirable for seismic interpretation, while the spectral representation shows a dominant frequency band consistent with the bandwidth of the processed seismic data. The extracted wavelet was subsequently used in the generation of synthetic seismograms and AVO responses, ensuring consistency between the seismic data and the modelling results.

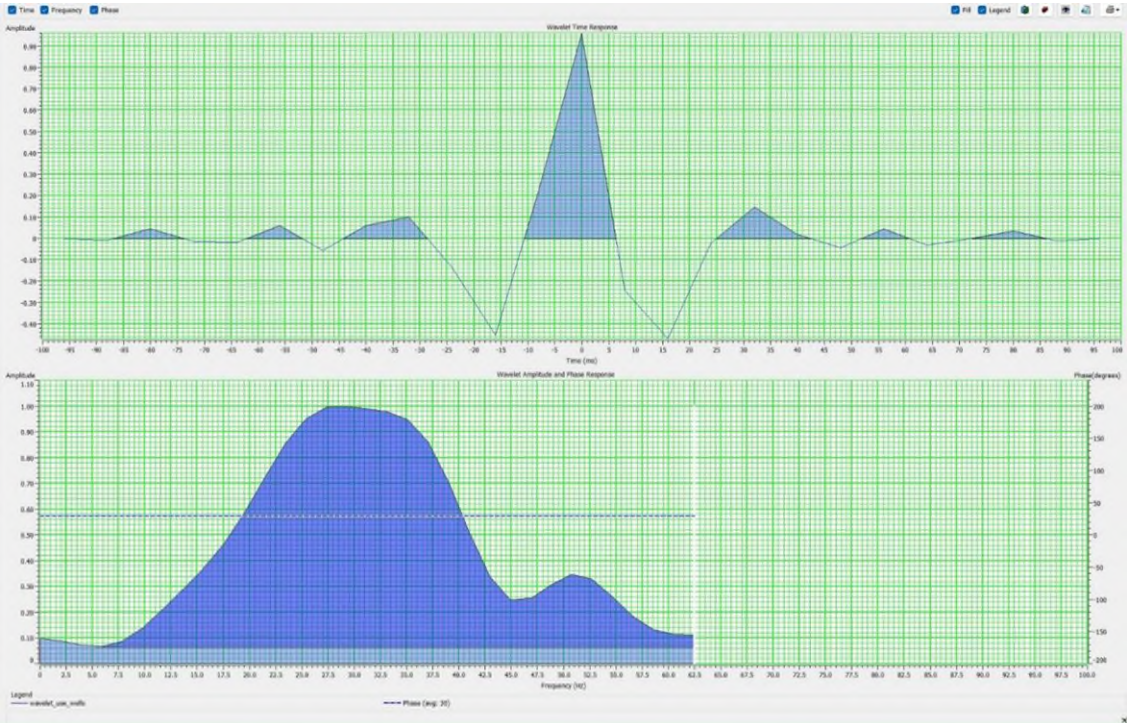


Fig. 7: Result of extracted statistical wavelet from CDP (a) The wavelets in time format. (b)The wavelet in spectra format

The final stage of the AVO modelling involved the generation of AVO synthetics using the fluid replacement modelling (FRM) derived elastic parameters for different fluid scenarios. Fig. 8 presents the results of the AVO synthetic generation, showing the modeled seismic responses corresponding to in-situ, oil-, gas-, and brine-filled conditions. Variations in amplitude and waveform character across offsets reflect changes in elastic contrasts driven primarily by fluid substitution effects. These results demonstrate the sensitivity of the reservoirs to fluid content and provide a quantitative basis for AVO interpretation, fluid discrimination, and subsequent seismic attribute analysis within the study area.

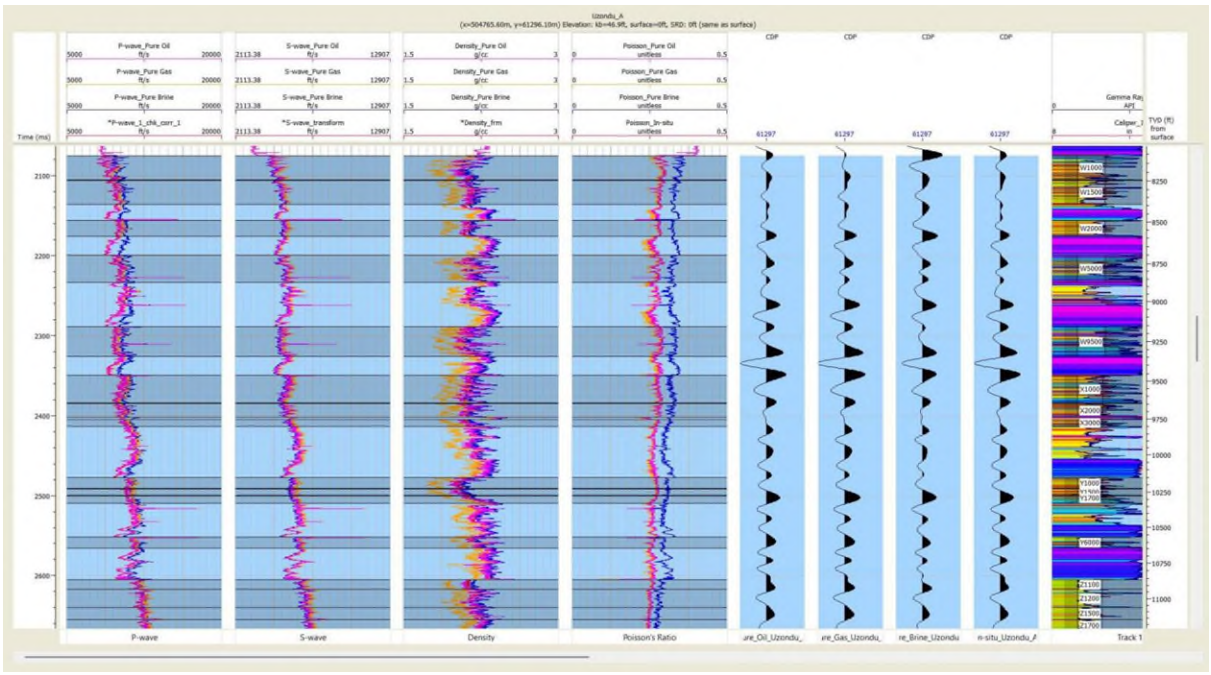


Fig. 8: Results of the AVO Synthetics generation

4.2 Results of the Post-stack Model

The post-stack elastic models show a quantitative description of the spatial variation of elastic properties across the study area and within the reservoir interval bounded by Horizon 1 and 3 (reservoir tops) and Horizon 3 and 4 (reservoir bases). These models are constrained by seismic data, well control, and fluid replacement modelling results, and they allow direct assessment of reservoir quality and continuity in terms of impedance, velocity, and density contrasts.

The S-impedance (Zs) model (Fig. 9) displays values ranging approximately from about 2,000 to 18,500 ft/s·g/cc, as indicated by the legend. Within the reservoir interval (reservoir A and B) between Horizon 1 & 3 and Horizon 3 & 4, Zs values are generally lower, typically in the range of ~9,000 to13,000 ft/s·g/cc, compared to the underlying formations where values increase beyond ~14,000 ft/s·g/cc. This reduction in S-impedance reflects decreased shear rigidity associated with porous, hydrocarbon-bearing sandstone. The relatively uniform lateral distribution of these lower Zs values across the section suggests good reservoir continuity.

The P-impedance (Zp) model (Fig. 10) shows a broader range of values, approximately 11,500 to 31,500 ft/s·g/cc. The reservoir interval (reservoir A and B) is characterized by comparatively lower to moderate Zp values, typically around ~21,000 to 24,000 ft/s·g/cc, relative to the overburden and deeper sections where Zp exceeds ~26,000 ft/s·g/cc. This impedance contrast is sufficient to generate strong seismic reflections at the reservoir boundaries and is consistent with the presence of hydrocarbon-saturated sandstone.

The Poisson's ratio model (Fig. 11) varies approximately between 0.23 and 0.48. Within the reservoir zone (reservoir A and B), Poisson's ratio values are generally lower, commonly in the range of ~0.30 to 0.36, compared to the overlying and underlying intervals where values exceed ~0.40. The reduced Poisson's ratio within the reservoir is indicative of hydrocarbon saturation, as fluids such as oil and gas tend to lower compressional compliance relative to shear response. This contrast further supports the interpretation of the reservoir interval as hydrocarbon-bearing.

The synthetic model (Fig. 12) reproduces the main reflection character observed in the seismic data, with amplitudes ranging between −1 and +1 (normalized seismic amplitude). The synthetic reflections show good alignment with the picked horizons, particularly at the reservoir top and base, indicating that the post-stack elastic parameters adequately capture the impedance contrasts responsible for the observed seismic response.

The density model (Fig. 13) shows density values ranging approximately from 1.9 to 2.5 g/cc. Within the reservoir interval, density values are moderate, typically ~2.1 to 2.3 g/cc, consistent with porous sandstone saturated with hydrocarbons. Higher densities exceeding ~2.35 g/cc are observed below Horizon 4, reflecting increased compaction and reduced porosity. The density contrast across the reservoir boundaries contributes significantly to the P-impedance variations and the resulting seismic reflectivity.

The quantitative post-stack modeling results consistently identify the interval between Horizon 1 and 3 and Horizon 3 and 4 as a laterally continuous reservoir characterized by lower S- and P-impedance, reduced Poisson's ratio, and relatively lower density compared to surrounding formations. These elastic property ranges collectively support the interpretation of a hydrocarbon-bearing sandstone reservoir and provide a robust foundation for further seismic inversion, reservoir characterization, and volumetric assessment.

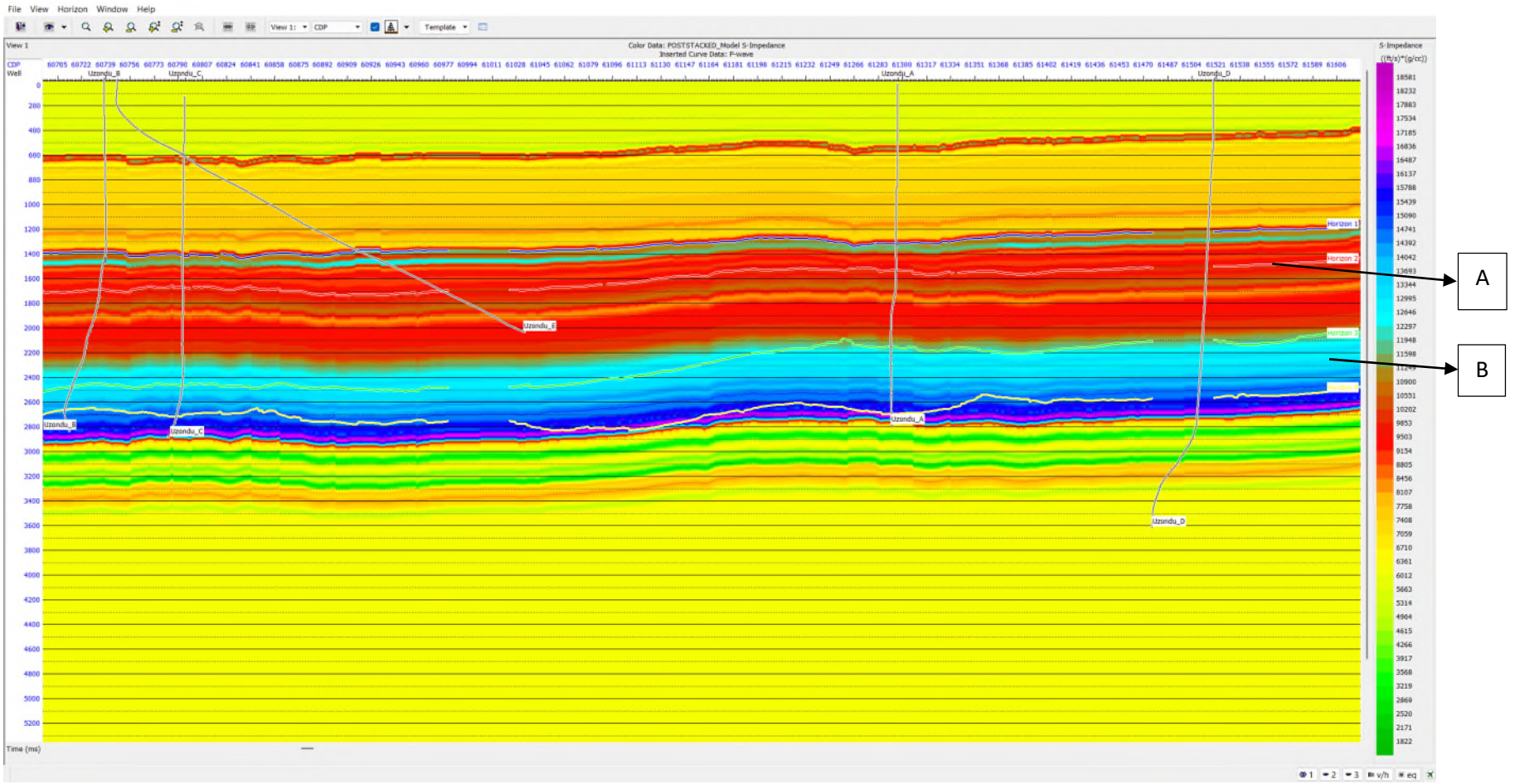


Fig. 9: Result of S-Impedance(Zs) model

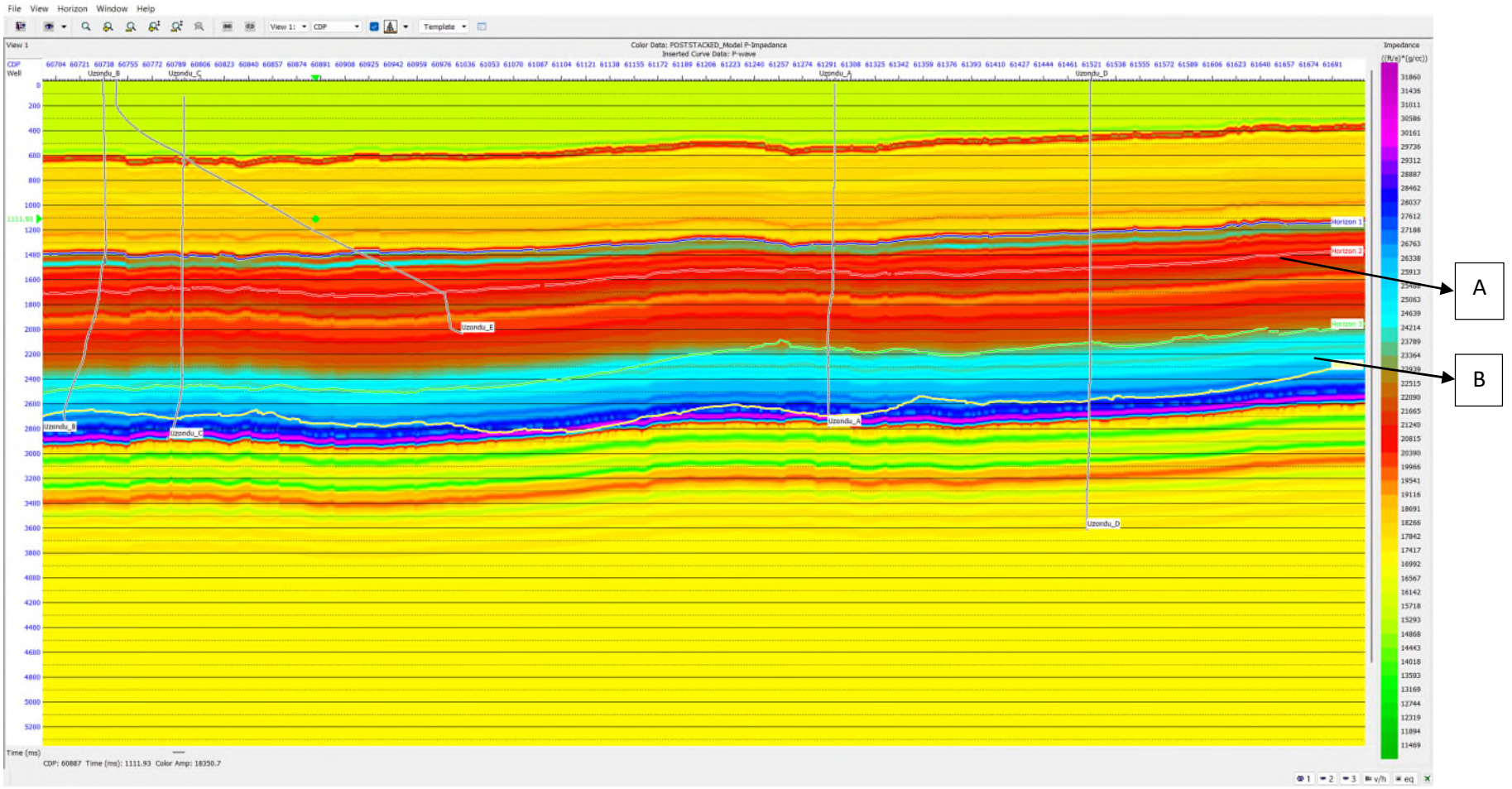


Fig. 10: Result of P-Impedance(Zp) model

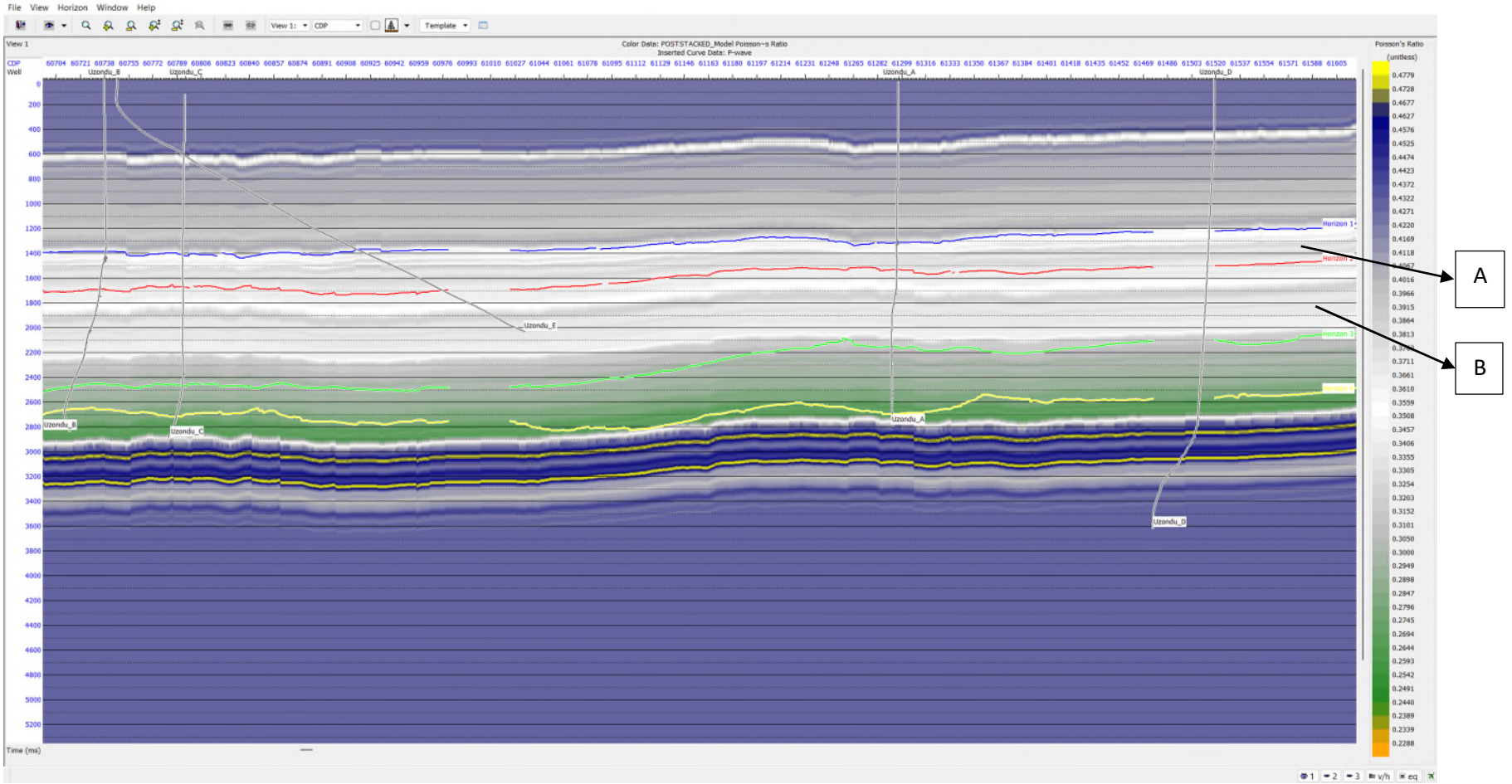


Fig. 11: Possion Ratio model

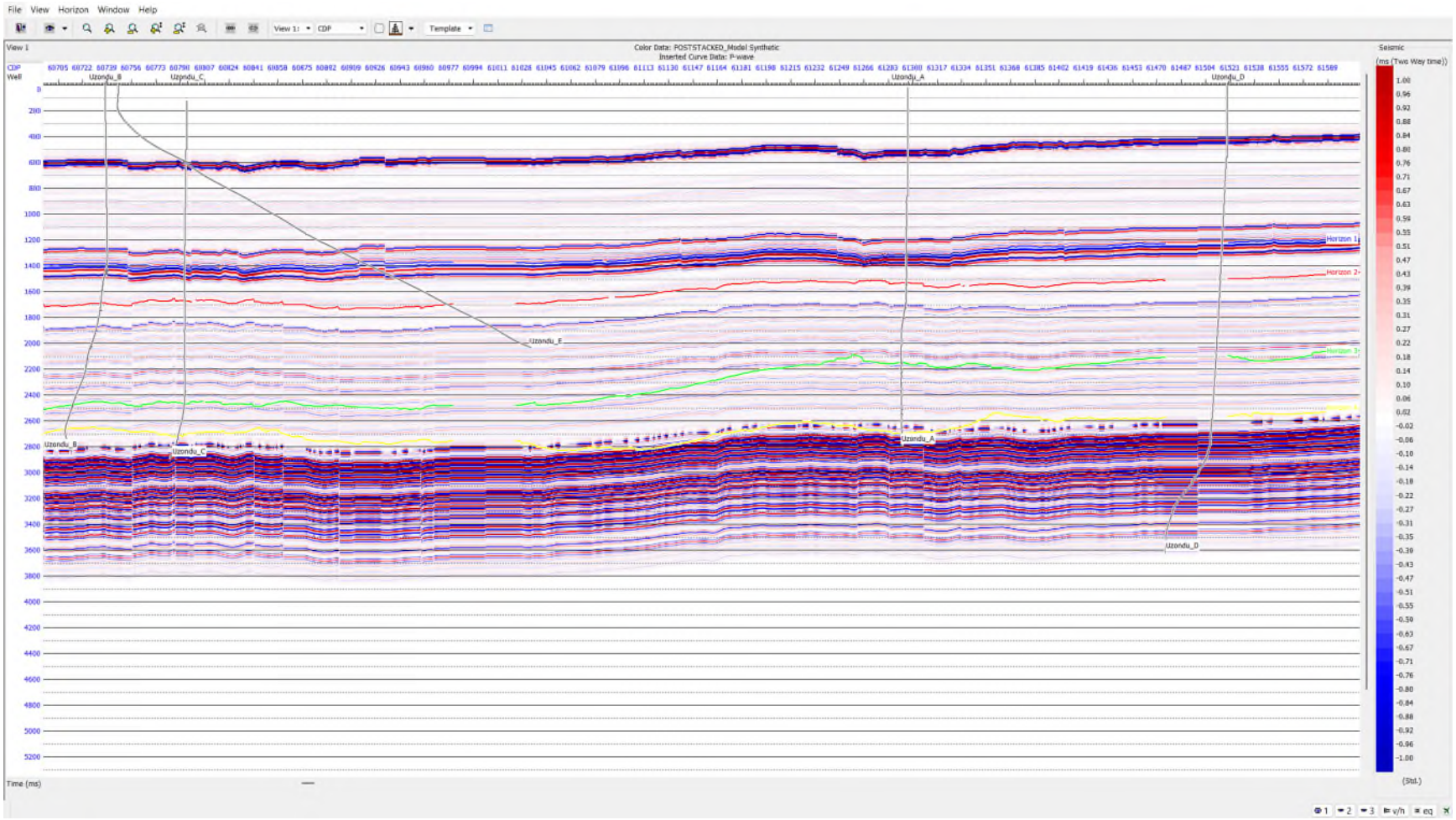


Fig. 12: Synthetic model

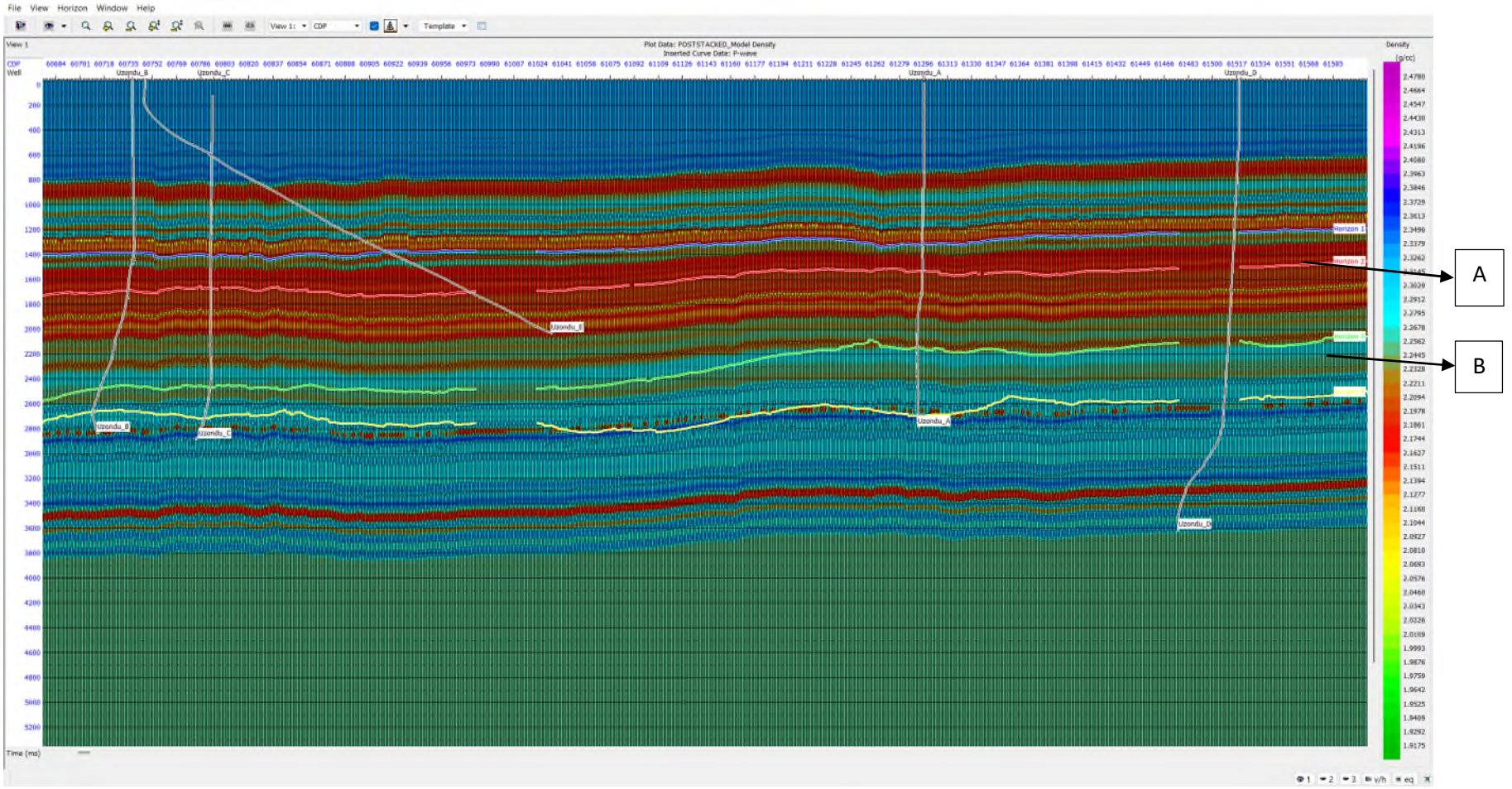


Fig. 13: Density model

5. CONCLUSTION

This study confirms that integrating seismic modelling with well data provides a reliable approach for resolving reservoir architecture in the *Uzondu* Field. Beyond identifying elastic contrasts, the workflow establishes a consistent seismic–well framework that enhances confidence in horizon mapping and subsurface interpretation.

The observed spatial distribution of elastic properties points that the reservoir bodies are not only continuous but also sufficiently thick and laterally extensive to support potential hydrocarbon accumulation and field development. Importantly, the study demonstrates that combining AVO modelling with fluid replacement techniques improves the sensitivity of seismic data to fluid effects, allowing clearer distinction between lithology-driven and fluid-driven responses. This reduces ambiguity commonly associated with amplitude-based interpretation in complex settings like the Niger Delta. The workflow provides a practical basis for improving reservoir prediction and supporting decision-making in hydrocarbon exploration and production.

DECLARATIONS

Ethical Approval: Not applicable.

Consent to Participate: Not applicable.

Consent to Publish: Not applicable.

Clinical Trial Registration: Not applicable. This study does not involve any clinical trials.

Data Availability: Dataset analyed for the study are available upon request from the corresponding author.

Conflict of Interest: The authors declare that they have no conflicts of interest.

Acknowledgments: The authors are grateful to Shell Petroleum Development Companies in Nigeria (SPDCN) for provision of the data that was used for this research work.

Funding statement: There was no funding of any sort received for this work.

References

[1] Short, KC; Stauble, AJ (1967). Outline of geology of Niger Delta. *AAPG Bulletin,* 51(5): 761–779. **DOI:**https://doi.org/10.1306/5D25C0CF-16C1-11D7-8645000102C1865D

[2] Weber, K. J., and Daukoru, E. M. (1975). Petroleum Geology of the Niger Delta. *Jour. Min. Geol.,* 12, 9-12

[3] Doust, H., and Omatsola, E. (1990). Niger Delta. In Divergent Passive Margin Basins *AAPG Memoir 48:* 201–238. **DOI:** https://doi.org/10.1306/M48508C4
[4] Evamy, BD; Haremboure, J; Kamerling, P; Molloy, FA; Rowlands, PH (1978). Hydrocarbon habitat of Tertiary Niger Delta. *AAPG Bulletin*, 62(1): 1–39. **DOI:** 10.1306/C1EA47ED-16C9-11D7-8645000102C1865D
[5] Corredor, F., Shaw, J. H., and Bilotti, F. (2005). Structural styles in the deep-water fold and thrust belts. *AAPG Bulletin*, 89(6): 753–780. **DOI:** https://doi.org/10.1306/02170504074
[6] Wojcik, K. M., Espejo, I. S., Kalejaiye, A. M., and Umahi, O. K. (2016). Bright spots, dim spots: Geologic controls of direct hydrocarbon indicator type, magnitude, and detectability, Niger Delta Basin. *Interpretation,* 4(3), 1–13. https://doi.org/10.1190/INT-2016-0062.1
[7] Allo, O. J., and Ogundimu, T. S. (2024). Seismic Attribute Analysis for Hydrocarbon Prospecting in the Agbada Formation of "Zee" Field, Niger Delta Basin. *FUDMA Journal of Sciences.*
[8] Attouman, K.D.B., Adeleye, M.A., Osinowo, O.O. (2025). Reservoir description and modelling using integrated seismic and petrophysical data in AKDB-field, offshore Niger delta, Nigeria. *Discov Geosci* **3**, 176 (2025). https://doi.org/10.1007/s44288-025-00292-6
[9] Oyedele, K. F and Ogagarue, D. O. (2013). Integration of 3D Seismic and Well log Data In the Optimal Reservoir Characterisation of EMI Field, Offshore Niger Delta Oil Province, Nigeria. *American Journal of Scientific and Industrial Research,* vol. 4, no. 1, pp. 11–21, 2013.
[10] Omoja, UC; Obiekezie, TN (2019). Application of 3D seismic attribute analyses for hydrocarbon prospectivity in Uzot-Field, onshore Niger Delta Basin, Nigeria. *Intern. J. Geophy.* 2019: 1-11 **DOI:** https://doi.org/10.1155/2019/1706416
[11] Russell, B. H. and Hampson, D. (1991). Comparison of poststack seismic inversion methods. *SEG* https://doi.org/10.1190/1.1888870
[12] Eze, S., Orji, O. M., Nnorom, S. L. and Ubogun, K. (2019) Model Based Inversion of Acoustic Impedance from Seismic Trace for Lithofacies Differentiation: an Application in Xy Field Offshore Niger Delta *J. Appl. Sci. Environ. Manage.* 23(9) 1677-1684
[13] Avseth, P; Mukerji, T; Mavko, G (2005). *Quantitative seismic interpretation: Applying rock physics tools to reduce interpretation risk*. Cambridge University Press. **DOI:**https://doi.org/10.1017/CBO9780511600074
[14] Doyen, P. M. (2007). *Seismic reservoir characterization:* An earth modelling perspective. EAGE Publications. https://doi.org/10.3997/9789462820234
[15] Bosch, M., Mukerji, T., Gonzalez, E.F., 2010. Seismic inversion for reservoir properties combining statistical rock physics and geostatistics: a review. Geophysics 75, 75A165–75A176. https://doi.org/10.1190/1.3478209.
[16] Chen, F., Zong, Z., Yin, X., 2024a. Seismic scattering inversion for multiple parameters of overburden-stressed isotropic media. Geophysics 89, T319–T336. https://doi.org/10.1190/geo2023-0636.1.
[17] Hosseinzadeh, S., Kadkhodaie, A., Mossadegh, H., Ilkhchi, R.K., 2019. Pore throat size characterization of carbonate reservoirs by integrating core data, well logs and seismic attributes. Geopersia 9, 395–410. https://doi.org/10.22059/ GEOPE.2019.269872.648430.
[18] Sabouhi, M., Kadkhodaie, A., Hosseinzadeh, S., Batezelli, A., 2024. Seismic sequence stratigraphy of late Albian-early Turonian successions in SW Iran: implication for reservoir characterizations and potential for improved reservoir

quality prediction. J. African Earth Sci. 214, 105269. https://doi.org/10.1016/j.jafrearsci.2024.105269.
[19] Wei, C., Xue-Bao, G., Feng, T., Ying, S., Wei-Hong, W., Hong-Ri, S., Xuan, K., 2021. Seismic velocity inversion based on CNN-LSTM fusion deep neural network. Appl. Geophys. 18, 499–514. https://doi.org/10.1007/s11770-021-0913-3.
[20] Hosseinzadeh, S., Abdollahi, R., Salimzadeh, S., Haghighi, M., 2024a. Three-dimensional coupled temporal geomechanical model for fault-reactivation and surfacedeformation evaluation during reservoir depletion and CO2 sequestration, securing long-term reservoir sustainability. Sustainability 16, 8482. https://doi.org/10.3390/su16198482.
[21] Jia, W., Zong, Z., Lan, T., 2023. Elastic impedance inversion incorporating fusion initial model and kernel Fisher discriminant analysis approach. J. Petrol. Sci. Eng. 220, 111235. https://doi.org/10.1016/j.petrol.2022.111235.
[22] Rawlinson, N., Fichtner, A., Sambridge, M., Young, M.K., 2014. Seismic Tomography and the Assessment of Uncertainty, pp. 1–76. https://doi.org/10.1016/bs. agph.2014.08.001.
[23] Khatibi, S., Aghajanpour, A., Ostadhassan, M., Farzay, O., 2018. Evaluating SingleParameter parabolic failure criterion in wellbore stability analysis. J. Nat. Gas Sci. Eng. 50, 166–180. https://doi.org/10.1016/j.jngse.2017.12.005.
[24] Alabi, A., and Enikanselu, P. A. (2019). Integrating seismic acoustic impedance inversion and attributes for reservoir analysis over 'DJ' Field, Niger Delta. *Journal of Petroleum Exploration and Production Technology,* 9, 2487–2496. DOI:10.1007/s13202-019-0720-z
[25] Oyedele, K. F., Olatinsu, O. B., Ige-Adeyeye, A. A., and Obasoro, O. A. (2020). Seismic impedance inversion and attribute analysis for reservoir characterization in an offshore depobelt, Niger Delta, Nigeria. *SN Applied Sciences,* 2, 1757. https://doi.org/10.1007/s42452-020-03571-8
[26] Akpan, A. S., · Okeke,·F. N., Obiora, D. N. and George, N. J (2021). Modelling and mapping hydrocarbon saturated sand reservoir using Poisson's impedance (PI) inversion: a case study of Bonna feld, Niger Delta swamp depobelt, Nigeria *Journal of Petroleum Exploration and Production Technology* 11:117–132
[27] Falade, A. O., Amigun, J. O., and Abiola, O. (2024). Hydrocarbon prospective study using seismic inversion and rock physics in an offshore field, Niger Delta. *Discover Geoscience,* 2, Article 24. https://doi.org/10.1007/s44288-024-00030-4
[28] Adesanya, O. Y., Adeoti, L., Oyedele, K. F., Afinotan, I. P., Oyeniran, T. and Alli, S. (2021) Hydrocarbon reservoir delineation using simultaneous and elastic impedance inversions in a Niger Delta field. *J. Petrol. Explor. Prod. Technol.* 11: 2891–2904. **DOI:** https://doi.org/10.1007/s13202-021-01191-5
[29] Oguka,V. O. Emujakporue G. O. and Balogun, A. O. 2023 Integration of AVO Analysis and Seismic Inversion for Reservoir Characterization of an Oil Field, Niger Delta, Nigeria. Asian J. Geol. Res.,vol. 6, no. 1, pp. 37-57, 2023;
[30] Ohakwere-Eze, M. C (2021). Reservoir Characterization Using Avo Analysis And Multiple Seismic Inversion In A Niger Delta Field, Nigeria. . Repository.mouau.edu.ng: Retrieved Oct 11, 2025, from https://repository.mouau.edu.ng/work/view/reservoir-characterization-using-avo-analysis-and-multiple-seismic-inversion-in-a-niger-delta-field-nigeria-7-2
[31] Gaber, Y., Ewida, H. F., Othman, A., and Ghazala, H. (2023). Post stack seismic data processing for enhancing subsurface reservoir mapping in the Shushan

basin, Western Desert, Egypt. *NRIAG Journal of Astronomy and Geophysics,* 12(1), 106–120. https://doi.org/10.1080/20909977.2023.2250970

[32] Omoja, U. C., Egwuonwu, G. N., Omonefe, F. and Okeugo, C. G. (2026a). Reservoir Quality Assessment Using Petrophysical Analysis in Uzondu Field, Niger Delta Basin. *Journal of Institutional Research, Big Data Analytics and Innovation* 2(1):135-151 https://doi.org/10.5281/zenodo.18904286

[33] Omoja, U. C., Egwuonwu, G. N., Omonefe, F. and Okeugo, C. G. (2026b). Elastic Property Variations of Hydrocarbon-Bearing Sandstones in Uzondu Field, Niger Delta Basin, Nigeria. *J. Appl. Sci. Environ. Manage.* 30 (3) 843-850 March 2026. https://www.ajol.info/index.php/jasem/article/view/321450

[34] Haack, RC; Sundararaman, P; Diedjomahor, JO; Xiao, H; Gant, NJ; May, ED; Kelsch, K (2000). Niger Delta petroleum systems, Nigeria, in M. R. Mello and B. J. Katz, eds., Petroleum systems of South Atlantic margins: *Am. Assoc. Petrol. Geol. Memoir.* 73: 213-231. **DOI:** https://doi.org/10.1306/M73705C16

[35] Weber, KJ (1987). Hydrocarbon distribution patterns in Nigerian growth fault structures controlled by structural style and stratigraphy: *J. Petro. Sci. Engr.* 1(2): 91-104 **DOI:** https://doi.org/10.1016/0920-4105(87)90001-5

[36] Castagna, JP; Batzle, ML; Eastwood, RL (1985). Relationships between compressional-wave and shear-wave velocities in clastic silicate rocks. *Geophys.* 50(4): 571–581. **DOI:** https://doi.org/10.1190/1.1441933

[37] Gassmann, F (1951). Elastic waves through a packing of spheres. *Geophy.* 16(4): 673–685.**DOI:** https://doi.org/10.1190/1.1437718